Published in final edited form as:
Cancer Res. 2007 April 1; 67(7): 3094–3105. doi:10.1158/0008-5472.CAN-06-3259.

E-Cadherin Cell-Cell Adhesion in Ewing Tumor Cells Mediates Suppression of Anoikis through Activation of the ErbB4 Tyrosine Kinase

Hyung-Gyoo Kang[1], **Jasmine M. Jenabi**[1], **Jingsong Zhang**[1], **Nino Keshelava**[2], **Hiroyuki Shimada**[1], **William A. May**[3], **Tony Ng**[4], **C. Patrick Reynolds**[2], **Timothy J. Triche**[1], and **Poul H.B. Sorensen**[1,4]

[1]Department of Pathology and Laboratory Medicine, Los Angeles, California

[2]Developmental Therapeutics Program, USC-CHLA Institute for Pediatric Clinical Research, Los Angeles, California

[3]Division of Hematology-Oncology, Children's Hospital Los Angeles, Los Angeles, California

[4]Department of Molecular Oncology, British Columbia Cancer Research Centre, Vancouver, British Columbia, Canada

Abstract

Ability to grow under anchorage-independent conditions is one of the major hallmarks of transformed cells. Key to this is the capacity of cells to suppress anoikis, or programmed cell death induced by detachment from the extracellular matrix. To model this phenomenon *in vitro*, we plated Ewing tumor cells under anchorage-independent conditions by transferring them to dishes coated with agar to prevent attachment to underlying plastic. This resulted in marked up-regulation of E-cadherin and rapid formation of multicellular spheroids in suspension. Addition of calcium chelators, antibodies to E-cadherin (but not to other cadherins or β_1-integrin), or expression of dominant negative E-cadherin led to massive apoptosis of spheroid cultures whereas adherent cultures were unaffected. This correlated with reduced activation of the phosphatidylinositol 3-kinase-Akt pathway but not the Ras-extracellular signal–regulated kinase 1/2 cascade. Furthermore, spheroid cultures showed profound chemoresistance to multiple cytotoxic agents compared with adherent cultures, which could be reversed by α-E-cadherin antibodies or dominant negative E-cadherin. In a screen for potential downstream effectors of spheroid cell survival, we detected E-cadherin–dependent activation of the ErbB4 receptor tyrosine kinase but not of other ErbB family members. Reduction of ErbB4 levels by RNA interference blocked Akt activation and spheroid cell survival and restored chemosensitivity to Ewing sarcoma spheroids. Our results indicate that anchorage-independent Ewing sarcoma cells suppress anoikis through a pathway involving E-cadherin cell-cell adhesion, which leads to ErbB4 activation of the phosphatidylinositol 3-kinase-Akt pathway, and that this is associated with increased resistance of cells to cytotoxic agents.

Keywords

suppression of anoikis; E-cadherin; ErbB4; EWS-FLI1; Ewing tumor

Requests for reprints: Poul H.B. Sorensen, Department of Molecular Oncology, British Columbia Cancer Research Centre, Room 4-112, Vancouver, British Columbia, Canada V5Z 1L4. Phone: 604-675-8202; Fax: 604-675-8218; psor@interchange.ubc.ca.

Introduction

Anchorage-independent growth refers to the ability of cells to survive and proliferate in the absence of attachment to the extracellular matrix (ECM). Normal nonhematopoietic cells typically undergo rapid cell death once such contacts are lost via a process known as anoikis (i.e., detachment-induced apoptosis; ref. 1). This likely prevents ectopic growth at inappropriate body sites. In contrast, anchorage-independent growth is a defining property of transformed cells (2), implicating resistance to anoikis as a key acquisition of malignant cells. Moreover, suppression of anoikis may be essential for metastatic spread of primary tumor cells (3, 4) because such cells must first detach from their local ECM and then enter and survive in the circulation before forming secondary tumors. Moreover, the concept of tumor dormancy holds that some malignant cells may persist in patients as quiescent cells that are resistant to therapy (5, 6). If, as hypothesized, such micrometastases survive within the circulation or bone marrow as small multicellular clusters or spheroids, then suppression of anoikis is likely also a key property of these cells. Elucidation of the molecular mechanisms of this process therefore has potentially profound relevance for targeting such cells therapeutically.

Growth within a three-dimensional environment is known to render cells less sensitive to exogenous apoptotic stimuli (7, 8). Mammary epithelial cells are more resistant to drug-induced apoptosis when grown in three-dimensional cultures such as ECM-containing Matrigel than in two-dimensional cultures (9 – 11), and integrin-ECM attachments are implicated in their increased survival (12). However, much less is known about how survival pathways are activated under anchorage-independent matrix-deficient conditions. The latter can be effectively modeled *in vitro* by culturing cells on agar-coated nonadherent plates, thus preventing attachment to plastic (13). Whereas most tumor cell lines form matrix-deficient multicellular spheroids under these conditions, nonmalignant cells generally fail to do so and undergo anoikis(14). Immortalized rat intestinal epithelial cells die rapidly in nonadherent cultures, but transfection of activated Ha-Ras results in survival of these cells as multicellular spheroids (15). Moreover, tumor spheroids show increased drug resistance compared with corresponding monolayers (16 – 18).

For epithelial cells, suppression of anoikis under matrix-deficient conditions seems to be induced through formation of cell-cell adhesions. For example, cadherin-mediated homotypic interactions support the survival of various epithelial cell types in the absence of ECM attachments (16, 19 – 22). Sequential disruption of cell-ECM and E-cadherin cell-cell contacts showed that the latter are critical for suppressing anoikis of normal enterocytes after detachment from villus epithelium (23). E-Cadherin also mediates survival of squamous carcinoma tumor spheroids (24). However, whether similar molecular mechanisms underlie anchorage-independent survival in nonepithelial tumors such as sarcomas remains unknown.

Here we have analyzed whether cell-cell adhesion and suppression of anoikis are also functionally related in sarcoma cells. We previously showed that when Ewing tumor (ET) sarcoma cells are transferred to nonadherent cultures, they rapidly form multicellular spheroids with ultrastructural evidence of cell-cell junctions (25). Spheroid formation correlated with an immediate block in cell proliferation and down-regulation of cyclin D1, the major D-type cyclin in ETs (26), although Ras-extracellular signal–regulated kinase (ERK)-1/2 and phosphatidylinositol 3-kinase (PI3K)-Akt pathways were activated (25). This suggested that cell-cell contacts in ET spheroids might activate signaling pathways in a manner favoring cell survival at the expense of cell growth. We now report that nonadherent ET cells up-regulate E-cadherin and form spheroids through E-cadherin–mediated cell-cell adhesion. This is associated with activation of the ErbB4 tyrosine kinase, induction of the PI3K-Akt pathway, and suppression of anoikis. Moreover, ET spheroids show broad

chemoresistance that can be reversed by inhibiting E-cadherin adhesion or down-regulating ErbB4 protein. This suggests a link between E-cadherin cell-cell contacts, ErbB4 activation, suppression of anoikis, and chemoresistance in anchorage-independent ET cells.

Materials and Methods

Cell lines and tissue culture

TC32 and TC71 ET cell lines and their growth requirements have previously been described (27). For anchorage-independent (spheroid) cultures, monolayer cells were trypsinized, resuspended as single cells, and replated at a concentration of 3.0×10^5/mL on standard dishes coated with 1.4% agar as described (25, 28).

Protein lysates, Western blotting, and immunoprecipitation

Harvested cells were rinsed in PBS containing 100 μmol/L Na_3VO_4 and lysed in NP40 lysis buffer (50 mmol/L HEPES, 100 mmol/L NaF, 10 mmol/L $Na_4P_2O_7$, 2 mmol/L Na_3VO_4, 2 mmol/L EDTA, 2 mmol/L $NaMoO_4$, and 0.5% NP40) containing a Roche protease inhibitor cocktail for 30 min at 4°C with shaking. Protein concentrations were standardized using detergent compatible Bio-Rad protein assay kits. Standard Western blot analysis was done with antibodies to poly(ADP-ribose) polymerase, phospho-Akt Ser^{473}, total Akt, phospho–mitogen-activated protein kinase/ERK kinase (MEK) 1/2 $Ser^{217/221}$ (Cell Signaling, Beverly, MA); β-actin, ErbB4, ErbB2 (Santa Cruz Biotechnology, Santa Cruz, CA); phospho-ErbB4 (Tyr^{1188}), phospho-ErbB2 (Tyr^{1112}) (Orbigen, San Diego, CA); E-cadherin, Rac1 (BD Transduction Laboratories, San Diego, CA); and phosphotyrosine (4G10 from Upstate, Lake Placid, NY). Secondary antimouse and antirabbit horseradish peroxidase (HRP)–conjugated antibodies were from BD Transduction Laboratories. For immunoprecipitation, whole-cell lysates were prepared as above and 1-mg cell lysates were precleared with protein G-agarose (Pierce, Rockford, IL) at 4°C for 1 h, incubated with indicated antibodies overnight at 4°C, and then incubated with protein G-agarose at 4°C for 1 h. Beads were collected by centrifugation and washed thrice with lysis buffer. Proteins were eluted by boiling in SDS sample buffer and subjected to immunoblotting with appropriate antibodies.

Treatment with drugs and signal transduction inhibitors

Cytotoxicity assays were done in 96-well tissue culture plates (for monolayers) and poly-2-hydroxyethyl methacrylate–coated 96-well plates (for spheroid cultures) using a semiautomated digital image microscopy scanning system (DIMSCAN), which has a dynamic range of 4 log of cell kill as described (29). Briefly, TC32 and TC71 cells were plated at 5,000/100 μL of complete medium per well. Cells were cultured for 1 day before addition of concentration ranges of carboplatin (0–10 mg/mL; Calbiochem, San Diego, CA), etoposide (0–10 mg/mL; Calbiochem), doxorubicin (0–100 ng/mL; Calbiochem), and topotecan (0–100 ng/mL; National Cancer Institute, Bethesda, MD) in replicates of 12 wells per condition. Plates were assayed 5 days after initiation of drug exposure. To measure cytotoxicity, fluorescein diacetate was added to plates at 10 μg/mL and incubated for 20 min. Then 30 μL of eosin-Y (0.5% in normal saline) were added to quench background fluorescence (29). Total fluorescence per well (after elimination of background fluorescence) was measured using a proprietary DIMSCAN system and results were expressed as the fractional survival of treated cells versus control cells. For apoptosis studies, spheroid and monolayer cells were treated with the above drugs, the MEK inhibitor U0126 (30 μmol/L; Calbiochem), the PI3K inhibitor LY294002 (20 μmol/L; Calbiochem), or DMSO vehicle control for 24 h. Harvested cells were then lysed with the NP40 lysis buffer and caspase-3 activity assay or Western blotting was done as indicated.

Inhibition of cell-cell adhesion using calcium chelators or blocking antibodies

Cells seeded at 10^5/mL in agar-coated six-well plates were treated ± 2.5, 5, or 10 mmol/L of EDTA or EGTA for 18 h at 37°C. Alternatively, cells treated ± 10 μg/mL mouse anti–E-cadherin (Zymed Laboratories, San Francisco, CA), 100 μg/mL anti–N-cadherin (Sigma, St. Louis, MO), 100 μg/mL anti–P-cadherin (Calbiochem), 50 μg/mL anti–OB-cadherin (R&D Systems, Minneapolis, MN), or 20 μg/mL anti–β_1-integrin (Chemicon, Temecula, CA) monoclonal antibodies were incubated for up to 48 h. Mouse anti-p21 monoclonal antibody (BD Transduction Laboratories), mouse immunoglobulin G1κ (Sigma), and goat IgG (Sigma) were used as controls.

DNA constructs, transfection, and selection of stable cell lines

A previously described dominant negative E-cadherin cDNA construct was a generous gift of Dr. Fiona Watt (London Research Institute, London, United Kingdom; ref. 30). The cDNA was subcloned into the pBabe-puromycin retroviral vector, and retroviral stocks were produced by transient transfection into the LinxA amphotrophic packaging line (Genetica, Boston, MA) as described (31). Stocks were used to transduce TC32 and TC71 cell lines, which were then selected in media containing 0.2 μg/mL puromycin. The wild-type mouse E-cadherin cDNA construct in pcDNA3 was a kind gift of Dr. Barbara Driscoll (Saban Research Institute, Los Angeles, CA). Cells were transfected using Lipofectamine 2000 (Invitrogen, Carlsbad, CA) and stable transfectants were selected in medium containing neomycin (800 μg/mL).

Soft agar colony assays

For soft agar assays, cells were seeded in triplicate at 2,000 per well of six-well plates as previously described (32). Plates were incubated for 14 days before being photographed and counted. Results shown are representative of at least three independent assays.

Caspase-3 assays

Caspase-3 activity was assayed by carbobenzoxy-Asp-Glu-Val-Asp-7-amino-4-trifluoromethyl coumarin (Z-DEVD-AFC) cleavage according to the manufacturer's protocols (Calbiochem). Briefly, cells grown under the indicated conditions were lysed as above at 4°C and lysates incubated with reaction buffer containing 50 μmol/L Z-DEVD-AFC. After 18 h at 37°C, fluorescence was measured with a GENiosPro instrument (Tecan, Grodig, Austria). Caspase-3 activity was adjusted for protein concentration and relative activity was expressed as the fluorescence ratio between the normalized caspase-3 activity of untreated cells (relative unit of 1.0) versus treated cells.

Immunofluorescence and immunohistochemistry

Monolayer cells grown on Lab-Tek II chamber slides were fixed with ethanol/acetone (1:1) and permeabilized with 0.1% Triton X-100 at room temperature for 30 min. Slides were incubated with N-cadherin, E-cadherin, and β-catenin antibodies (BD Transduction Laboratories) at 4°C for 2 h, followed by visualization with a Cy3-conjugated goat anti-mouse secondary antibody (Jackson ImmunoResearch, West Grove, PA). Slides were counterstained with Vectorshield (Vector, Burlingame, CA) containing 4′,6-diamidino-2-phenylindole and images were obtained using a Zeiss microscope with a SPOT Insight QE Camera. Spheroids were briefly washed in cold PBS, centrifuged at 700 rpm for 3 min, immersed in Tissue-Tek optimum cutting temperature compound (Sakura Finetek, Torrance, CA), and then frozen in isopentane in liquid nitrogen. Cryostat sections (10 μm) were fixed, permeabilized, stained, and imaged using standard methods. For immunohistochemistry, paraffin-embedded blocks of primary ET samples were obtained from the Children's Hospital Los Angeles tumor bank and immunohistochemistry was done with anti–ErbB-4

antibodies (1:100; Santa Cruz Biotechnology) or anti–E-cadherin antibodies (1:500; BD Transduction). Immunostaining was done using Benchmark (Ventana, Tucson, AZ) with biotinylated immunoglobulin, streptavidin-HRP, 3,3′-diaminobenzidine/H_2O_2, and copper. Counterstaining was done with hematoxylin before light microscopic examination.

Activated tyrosine kinase arrays

Monolayer and spheroid TC32 and TC71 cells were grown for 48 h in 10% serum–containing medium and transferred to 0.5% serum–containing medium for a further 24 h. Cells were then washed with PBS containing 100 μmol/L Na_3VO_4, solubilized in lysis buffer, and then 300 μg of total protein were incubated with Human Phospho-RTK Arrays (R&D Systems)[5] according to the manufacturer's protocols. Briefly, arrays were incubated with whole-cell lysates overnight at 4°C with shaking and washed with the supplied washing buffer. Arrays were then incubated with anti–phosphotyrosine-HRP antibodies for 2 h at room temperature on a rocking platform shaker before incubation with a chemiluminescent reagent and film exposure.

ErbB4 knockdown using small interfering RNAs

Two independent small interfering RNA (siRNA) oligonucleotide pools targeting ErbB4 were used to block ErbB4 expression. These included a previously described pool (5′-ACUGAGCUCUCUCUCUGACTT-3′ and 5′-GUCAGAGAGAGAGCUCAGUTT-3′; Eurogentec, San Diego, CA; ref. 33) and a commercially available SMARTpool of four siRNAs (Dharmacon, Chicago, IL). Double-stranded siRNAs (100 nmol/L) were transfected into adherent cells using Lipofectamine 2000 (Invitrogen) according to the manufacturer's protocols. Transiently transfected cells were grown for 24 h and replated on agar-coated six-well plates. After 24 h, cell extracts were generated as above and ErbB4 protein expression was analyzed using anti-ErbB4 antibodies (1:1,000; Santa Cruz Biotechnology). In some experiments, cells were treated with 50 μmol/L etoposide or 10 μmol/L doxorubicin for 18 h after siRNA transfection, and caspase-3 activity was assayed as above.

Results

ET spheroids suppress anoikis through the PI3K-Akt pathway

When transferred to nonadherent culture conditions, ET cell lines suppress anoikis and survive as multicellular spheroids (ref. 25; see also Supplementary Fig. S1*A*). We postulated that this effect might be mediated through either the Ras-ERK1/2 or PI3K-Akt cascade because both become activated in ET spheroids (25). To test this, we used two previously characterized ET cell lines, TC32 and TC71, each of which expresses the ET-specific *EWS-FLI1* gene fusion (25, 27). TC32 and TC71 monolayer and spheroid cultures were assessed for caspase-3 activation (to measure apoptosis) after treatment with the PI3K inhibitor LY294002 or the MEK inhibitor U0126. As shown in Fig. 1*A*, 20 μmol/L LY294002 increased caspase-3 activation in spheroids of both lines by > 2-fold (which correlated with < 25% viability; data not shown), whereas up to 30 μmol/L U0126 (or another MEK inhibitor, PD98059; data not shown) had virtually no effect. Corresponding monolayers were even more sensitive to PI3K inhibition, consistent with the well-established role of the PI3K-Akt cascade in adherent cell survival (34); monolayers also showed a slight response to MEK inhibition (Fig. 1A). A dose-response curve of LY294002 treatment versus caspase-3 activation confirmed the LY294002 effect over a wide concentration range in ET spheroids (Supplementary Fig. S1*B*). Moreover, significant cleavage of the caspase-3 substrate poly(ADP-ribose) polymerase in ET spheroids was observed with LY294002 treatment but not U0126 (Fig. 1*B*). Finally, spheroid formation was dramatically reduced by LY294002 but not U0126 (Fig. 1C). These results indicate that, similar to its effect on

monolayer cell survival, the PI3K-Akt pathway plays a major role in suppression of anoikis of ET spheroids.

Anchorage-independent growth induces E-cadherin–dependent cell-cell adhesion in ET spheroids

Because multicellular spheroids are thought to form through cell-cell adhesions (14), we hypothesized that such adhesions might also mediate suppression of anoikis in ET spheroids and sought to identify the adhesion molecules involved. Treatment of spheroid cultures with 2.5 to 10 mmol/L of the calcium-chelating agent EDTA (or EGTA; data not shown), which blocks cadherin and integrin engagement but maintains intracellular calcium levels (35), results in rapid dissociation of ET spheroids to single cells and dose-dependent caspase-3 induction (see Supplementary Fig. S2*A*). This suggested a role for calcium-dependent cell-cell adhesion involving integrins or cadherins in the formation/maintenance of ET spheroids. Based on Affymetrix gene expression profiling, β_1-integrin is the predominant integrin transcript expressed in ET cell lines whereas E-cadherin, N-cadherin, OB-cadherin, and P-cadherin transcripts are variably expressed (data not shown). To investigate the potential roles of these proteins in spheroid formation, we tested whether blocking antibodies to β_1-integrin or E-cadherin, N-cadherin, OB-cadherin, and P-cadherin could inhibit spheroid formation. Only anti–E-cadherin antibodies did so (Fig. 2A), and this correlated with rapid caspase-3 activation in TC32 and TC71 spheroids (Fig. 2B) but not in corresponding monolayers (data not shown). None of the other antibodies blocked spheroid formation (Supplementary Fig. S2), nor did addition of RGD peptides to inhibit β_1-integrin/ECM contacts (data not shown). Anti–β_1-integrin antibodies did block attachment of ET monolayer cultures to plastic, suggesting that β_1-integrin cell adhesion is important in ET monolayers.

E-Cadherin expression is up-regulated in ET spheroid cultures

We next compared E-cadherin expression in ET monolayer versus spheroid cultures. By Western blotting, E-cadherin levels were increased in spheroids under various conditions compared with corresponding monolayer cells (see Fig. 2C). This was confirmed by immunofluorescence staining; whereas N-cadherin levels were higher in monolayers, its expression was correspondingly reduced in ET spheroids and E-cadherin was increased (see Fig. 2D). E-Cadherin was clearly localized to cell-cell junctions in ET spheroids, but this was much less obvious in ET monolayer cells (Fig. 2*D*). Because E-cadherin surface expression can influence β-catenin cellular localization, we tested whether β-catenin was differentially localized in ET spheroid versus monolayer cells. However, β-catenin was predominantly localized to cell membranes in both spheroid and monolayer cells by immunofluorescence (Fig. 2*D*) or Western blotting after subcellular fractionation (data not shown). These results implicate E-cadherin in cell-cell attachments of ET spheroids, although we have not ruled out roles for other adhesion proteins in this process.

Dominant negative E-cadherin increases apoptosis and sensitivity of ET spheroids to PI3K inhibitors

We next tested whether a dominant negative form of E-cadherin or overexpression of wild-type E-cadherin in ET cell lines influences spheroid formation. A previously described dominant negative E-cadherin (DN-Ecad) construct encoding a 66-kDa chimeric protein with the H-2Kd extracellular domain linked to the transmembrane and cytoplasmic domains of E-cadherin (30), or one encoding wild-type E-cadherin (Ecad), was stably expressed in ET monolayer cells as shown in Supplementary Fig. S3*A*. These constructs had no phenotypic or other effects on monolayer growth (data not shown). However, following transfer to agar-coated plates, cell-cell aggregate formation was markedly diminished in

TC32 cells expressing DN-Ecad, both in short-term (6 h) and longer-term (30 h) nonadherent cultures (Supplementary Fig. S3*B*); this was particularly evident compared with cells overexpressing Ecad. We then tested whether this effect correlated with increased caspase-3 activation. Whereas DN-Ecad expression had no effects on monolayer cells (see Fig. 3*A*), DN-Ecad–expressing TC32 and TC71 spheroid cells showed > 2-fold higher caspase-3 activation over 24 h compared with control spheroids (nontransduced, vector alone, or Ecad) even in the presence of serum, and these cells were dramatically more sensitive to serum deprivation or LY294002 treatment. Addition of the U0126 MEK inhibitor had little or no effect on caspase-3 activation in DN-Ecad–expressing spheroids (data not shown).

To confirm that the inhibitory action of DN-Ecad on spheroid growth mainly targeted the PI3K-Akt pathway as opposed to Ras-ERK1/2, the activation state of these cascades by DN-Ecad cells was examined. As shown in Fig. 3*B*, both TC32 and TC71 cells expressing DN-Ecad showed a marked decrease in Akt Ser^{473} phosphorylation compared with nontransduced, vector alone, or Ecad-expressing cells, whereas there was no inhibitory effect on MEK activation. Interestingly, DN-Ecad also slightly blocked Akt activation in ET monolayer cultures at high confluence (>90%) but not at lower confluence (<70%; data not shown), suggesting that limited E-cadherin cell-cell contacts may also occur in confluent monolayer cells. Finally, we compared soft agar colony formation of each cell line as a further measure of anchorage-independent growth. As seen in Fig. 3*C* and *D*, DN-Ecad cells formed fewer and significantly smaller colonies compared with nontransduced or vector alone cells, whereas Ecad-expressing cells showed a tendency for increased colony formation. Taken together, these results strongly support a role for E-cadherin in the survival of anchorage-independent ET cells and further suggest that the PI3K-Akt pathway is central to this process.

ET spheroids show widespread E-cadherin–dependent chemoresistance

Because spheroid growth is reported to confer chemoresistance to tumor cell lines (16 – 18), we wondered whether suppression of anoikis in ET spheroids might be also linked to altered chemosensitivity. We therefore determined cytotoxicity profiles of selected chemotherapeutic agents in monolayer versus spheroid cultures of TC32 and TC71 ET cell lines using the DIMSCAN drug sensitivity screening platform (29). Spheroid cultures of both cell lines were consistently more resistant to carboplatin (as measured by cellular fractional survival) compared with corresponding monolayers across a broad concentration range (see Fig. 4*A*). Identical patterns were observed with etoposide, melphalan, doxorubicin, or topotecan(Fig. 4*B*). A possible caveat of these studies is that drug diffusion to central cells of spheroids might be physically attenuated compared with monolayer cells. However, in previous studies using similar time courses, penetration of bromodeoxyuridine was not limited to outer cells but was equally distributed throughout ET spheroids (25, 28). Therefore, drug penetration is unlikely to be a limiting factor under these conditions. If, instead, chemoresistance is functionally related to suppression of anoikis in ET spheroids, then blocking cell-cell adhesions should restore chemosensitivity. To investigate this, we compared caspase-3 activation in spheroid cultures of the ET cell lines expressing the above E-cadherin constructs. Spheroids were treated with doxorubicin and etoposide, two anticancer drugs used in the treatment of ETs, and caspase-3 activation was monitored. As shown in Fig. 4*C*, expression of DN-Ecad clearly increased the chemosensitivity of TC32 and TC71 spheroids to doxorubicin or etoposide, particularly for TC71 cells. Moreover, E-cadherin–overexpressing cells showed increased resistance to these drugs compared with controls. In contrast, expression of DN-Ecad did not significantly influence chemosensitivity of ET monolayer cells (Supplementary Fig. S3*C*). These results strongly indicate that E-cadherin cell-cell contacts can influence chemosensitivity of ET spheroids.

Analysis of E-cadherin downstream signaling pathways reveals a role for ErbB4 in ET spheroid survival

We next wished to determine the molecular mechanisms by which E-cadherin modulates spheroid survival. E-Cadherin is known to activate cell signaling through at least three different mechanisms, including the β-catenin/Wnt pathway, Rho GTPases, and receptor tyrosine kinases (RTKs; ref. 31). We therefore tested whether any of these downstream pathways are involved in E-cadherin–mediated survival of ET spheroids. As shown above in Fig. 2*D*, β-catenin was localized to membranes by immunofluorescence in both ET monolayers and spheroids, and β-catenin could not be detected in the cytoplasm or nucleus by immunostaining in either culture system (data not shown). Moreover, T-cell factor/lymphoid enhancer-binding factor reporter assays failed to show β-catenin–dependent transcriptional regulation in ET spheroids (data not shown). Although not ruling out a role for β-catenin activation, our results do not favor this as a major mechanism for ET spheroid survival. To investigate the potential activation of Rho GTPases by E-cadherin engagement, we did pull-down assays of activated Rac1, Cdc42, and RhoA. Although we found increased Rac1 and Cdc42 activation in ET spheroids compared with monolayers, we could not show a direct relationship to E-cadherin expression levels (data not shown). Therefore, the role of Rho GTPases in this process awaits further analysis.

To screen for activation of specific RTKs in ET spheroids, we used the R&D Systems Human Phospho-RTK Antibody Proteome Profiler Array of 42 different tyrosine kinases.[6] Lysates from TC32 and TC71 cell lines grown in low serum showed differential activation of several RTKs in spheroids compared with monolayers, most prominently ErbB4 (see Fig. 5*A*). To validate this, lysates were subjected to immunoprecipitation with anti-phosphotyrosine antibodies followed by total ErbB4 immunoblotting(Fig. 5*B*, *top*). This showed increased tyrosine phosphorylation of a major 180-kDa band, the expected size of ErbB4, and a less prominent 80-kDa band in TC32 and TC71 spheroids versus monolayers. Activated ErbB4 can be proteolytically cleaved to generate a soluble 80-kDa cytosolic fragment, ErbB4-s80, which retains tyrosine kinase activity (36 – 38), and we hypothesized that the 80-kDa band represents ErbB4-s80. Western blots of input lysates using total ErbB4 antibodies showed similar expression of the 180-kDa ErbB4 protein in spheroids versus monolayers, whereas the 80-kDa band was not readily apparent (Fig. 5*B*, *top*). Therefore, to validate the above results, a reciprocal experiment was done in which ErbB4 immunoprecipitations were followed by anti-phosphotyrosine immunoblottings. This showed enhanced tyrosine phosphorylation of the same 180- and 80-kDa bands in ET spheroids (Fig. 5*B*, *bottom left*), which were confirmed to represent ErbB4 by reprobing with total ErbB4 antibodies (Fig. 5*B*, *bottom right*). Furthermore, using a previously described phospho-Tyr^{1188} specific antibody to detect activated ErbB4 (39), Western blotting clearly showed increased tyrosine phosphorylation of both ErbB4 180-kDa and s80 forms in ET spheroids compared with monolayers (Fig. 5*C*). Finally, to verify ErbB4 protein expression in primary ETs, we did immunohistochemistry on five *EWS-ETS* gene fusion–positive ET tumors. This showed strong ErbB4 expression in all five cases, with both a membranous and cytosolic staining pattern (shown for three representative cases in Fig. 5*D*). Taken together, these results strongly indicate that ErbB4 is expressed in primary ETs, and that this RTK is preferentially activated in ET cell line spheroids compared with monolayers. Although the significance of ErbB4-s80 expression remains to be determined, its demonstration provides additional evidence for ErbB4 activation in ET spheroids.

The above protein array studies also suggested activation of ErbB2 in ET spheroids (Fig. 5*A*). However, when ErbB2 was immunoprecipitated from cell lysates and immunoblotted with anti-phosphotyrosine antibodies, more activation was detected in TC32 monolayers compared with spheroid cells (Supplementary Fig. S4*B*). Identical results were found for

TC71 cells (data not shown). Expression of all four ErbB family members in TC32 and TC71 cells was also assessed by quantitative reverse transcription-PCR. This showed relative transcript levels as follows: glyceraldehyde-3-phosphate dehydrogenase control > ErbB2 > ErbB4 > ErbB3 ≫ ErbB1, with ErbB1 expression being virtually undetectable (data not shown). Therefore, whereas ErbB2 and ErbB4 are both expressed in TC32 and TC71 cells, the latter is preferentially activated in spheroids.

DN-Ecad expression blocks ErbB4 activation

We next assessed whether ErbB4 activation in ET spheroids correlates with functional E-cadherin expression. Using the above phospho-specific ErbB4 antibodies, we observed that ErbB4 activation was markedly reduced in ET spheroids when DN-Ecad was expressed, whereas it was enhanced in spheroids overexpressing E-cadherin (Fig. 6*A*). DN-Ecad also reduced ErbB4 activation in confluent ET monolayers, suggesting as above that limited E-cadherin cell-cell contacts may occur in monolayers under high cell density. In contrast, DN-Ecad expression did not influence ErbB2 activation in spheroids (Supplementary Fig. S4*C*), as measured with ErbB2 phospho-Tyr^{1112} specific antibodies (40). In fact, ErbB2 activation seemed to be reduced in spheroids compared with monolayers. These data provide strong evidence that ErbB4 activation is specifically linked to functional E-cadherin expression in ET spheroids. To determine E-cadherin expression in primary ETs, we did immunohistochemistry on the above five ET tumors. E-Cadherin expression ranged from strong membranous staining (see case 1, Fig. 5*D*) to virtually complete absence of staining (case 2, Fig. 5*D*), with the other cases showing intermediate staining consisting of a mixed membranous and cytosolic pattern (e.g., case 3, Fig. 5*D*). The significance of this variable pattern of E-cadherin staining in primary ETs remains to be determined.

ErbB4 knockdown inhibits Akt activation and restores chemosensitivity to ET spheroids

We next wished to determine whether reducing ErbB4 expression influences formation or survival of ET spheroids. TC32 cells were treated with either a DharmaconSMARTpool of four siRNAs directed against ErbB4 or a pool of two previously described siRNAs targeting different sequences of *ErbB4*(33) before transfer of cells to nonadherent cultures. As shown in Fig. 6*B*, both reagents effectively reduced ErbB4 protein levels by > 60% to 80% compared with scrambled controls (or nontransduced cells; data not shown). ET cells expressing either siRNA pool were still capable of forming spheroids, although these were reduced in size and number (Fig. 6*C*). ErbB4 knockdown using either pool correlated with marked loss of Akt activation in ET spheroids whereas there was no effect on MEK activation (Fig. 6*B*). Finally, whereas ErbB4 knockdown alone moderately increased caspase-3 activation in ET spheroids, this effect was dramatically enhanced in the presence of either etoposide or doxorubicin (Fig. 6*D*). In contrast, ErbB4 knockdown did not significantly affect chemosensitivity of ET monolayer cells (shown for TC32 in Supplementary Fig. S4*D*). These results are consistent with a model whereby ErbB4 activation leads to induction of PI3K-Akt in ET spheroids, and blocking ErbB4 may render these cells more sensitive to chemotherapeutic agents.

Discussion

The ability to suppress anoikis is a key acquisition of malignant cells and may be essential for the metastatic process (41) and tumor cell dormancy (42). It is generally thought that anoikis is initiated by loss of cell-ECM contacts (1) and that epithelial tumor cells compensate for this through formation of cell-cell contacts (16, 19 – 22). However, the corresponding molecular mechanisms in sarcomas remain unknown. This is an extremely important issue as most sarcoma-related deaths occur as a result of metastatic disease. We have now used ET spheroids as a model to study sarcoma anchorage-independent growth.

This revealed a novel pathway linking up-regulation of E-cadherin in ET spheroids to activation of the ErbB4 tyrosine kinase, stimulation of the PI3K-Akt cascade, and suppression of anoikis in ET cell lines.

We find that ET cells, when forced to grow under anchorage-independent conditions, up-regulate E-cadherin as a mechanism for suppressing anoikis. E-Cadherin is an epithelial cadherin and is not considered a marker for sarcomas other than those with epithelioid features such as synovial sarcoma (43, 44). However, E-cadherin expression has been reported in ETs (45), including recent studies linking its expression in ETs to caveolin-1 (46). Although E-cadherin is generally regarded as a tumor suppressor whose loss is associated with poor prognosis in epithelial tumors (31), several studies challenge this view. E-Cadherin is essential for anchorage-independent growth of oral squamous carcinoma cells (24), and its expression is maintained during disease progression (47). Normal ovarian surface epithelium expresses low E-cadherin levels, but expression increases in ovarian neoplasia including invasive tumors (48 – 50). Ectopically expressed E-cadherin suppresses anoikis in ovarian surface epithelial cells and supports their survival as aggregates in ascitic fluid (51). Therefore, certain epithelial cancers may express E-cadherin in advanced tumors to suppress anoikis, such as during metastatic spread. Our studies show variable E-cadherin expression in primary ETs and up-regulation in ET spheroids. It is intriguing to speculate that the ability to induce E-cadherin expression may be associated with anchorage-independent cell survival and metastatic potential in ETs.

Our results indicate that E-cadherin cell-cell contacts lead to activation of the ErbB4 RTK in ET spheroids. The opposite model, whereby ErbB4 activation is upstream of E-cadherin induction, is unlikely because cells treated with ErbB4 siRNAs show no difference in E-cadherin levels compared with controls (Supplementary Fig. 4*E*). Expression of ErbB4, an epidermal growth factor (EGF) receptor family member that binds neuregulin EGF-like ligands (52), has not been previously reported in ETs. The role of ErbB4 in transformation remains controversial (53), with evidence for both oncogenic (54, 55) and tumor suppressor activities (56, 57). This dichotomy may reflect divergent activity of ErbB4 alternatively spliced isoforms (33). ErbB4 activation leads to homodimerization or heterodimerization with other ErbB proteins, resulting in kinase activation and induction of multiple signaling pathways including Ras-ERK1/2 and PI3K-Akt. In preliminary studies, we failed to detect ErbB4 heterodimerization with other ErbB proteins (data not shown). ErbB4 activation also leads to a series of proteolytic cleavage steps. The tumor necrosis factor α–converting enzyme metalloproteinase first cleaves ErbB4 to generate membrane-bound ErbB4-m80, which is further cleaved by γ-secretase to generate a cytosolic 80-kDa protein tyrosine kinase–containing protein, s80 (36, 37). The s80 fragment functions as a constitutively active tyrosine kinase (38) and can translocate to the nucleus. Whereas we observe that a tyrosine phosphorylated s80 form is preferentially generated in ET spheroids (Fig. 5*B* and *C*), whether this functions in suppression of anoikis remains unknown. It is also unclear how E-cadherin cell-cell contacts might activate ErbB4 in ET spheroids. One possibility is that E-cadherin induces autocrine neuregulin expression, although we currently have no evidence for this. An alternative mechanism is suggested by a recent report that in oral squamous carcinoma cells, E-cadherin–mediated suppression of anoikis is associated with ligand-independent activation of ErbB1 through a direct surface interaction between these proteins (58). Although not tested, recruitment of E-cadherin/ErbB1 complexes to cell junctions resulting in localized ErbB1 oligomerization was proposed as a mechanism of kinase activation. E-Cadherin cell-cell contacts have also been associated with activation of ErbB1 in HaCaT cells (59) and EphA2 in breast cancer cells (60). It is therefore conceivable that a similar mechanism occurs in ET cells, with direct activation of ErbB4 through E-cadherin/ErbB4 complex formation. Studies to address this are under way.

In ET spheroids, E-cadherin expression and ErbB4 activation both correlated with PI3K-Akt induction whereas the Ras-ERK1/2 pathway was unaffected. Moreover, PI3K inhibitors were highly active in blocking ET spheroid survival whereas MEK inhibitors were not. This indicates that the PI3K-Akt pathway is critical for suppression of anoikis in ET spheroids. We recently found that in mouse embryo fibroblasts transformed by the ETV6-NTRK3 chimeric tyrosine kinase, an intact insulin-like growth factor I receptor axis is essential for suppression of anoikis as it is required for induction of PI3K-Akt but not Ras-ERK1/2 (28). Similarly, the TrkB RTK suppresses anoikis in rat intestinal epithelial cells through activation of the PI3K-Akt pathway, and TrkB conferred the ability of rat intestinal epithelial cellular aggregates to colonize distant organs (4). In contrast, suppression of anoikis in ovarian carcinoma cells through E-cadherin–mediated activation of ErbB1 requires induction of the Ras-ERK1/2 cascade but not PI3K-Akt (58). Moreover, other pathways such as Janus-activated kinase-signal transducers and activators of transcription-3 signaling are also implicated in anchorage-independent growth (61). It is therefore likely that cell context is important for determining the exact molecular mechanisms used for this process (1, 41). The common theme is that the activation of tyrosine kinases by cell-cell adhesion may be critical for suppression of anoikis in tumor cells.

ET spheroids showed increased resistance to multiple chemotherapeutic agents compared with corresponding monolayer cultures, and reducing E-cadherin cell-cell contacts or ErbB4 levels restored chemosensitivity. E-Cadherin blocking antibodies also sensitized human colorectal carcinoma cells to chemotherapy (62), in keeping with many reports linking growth of tumor cells under anchorage-independent conditions to widespread chemoresistance (16 – 18). It is tempting to speculate that these phenomena are related (i.e., activation of anti-anoikis pathways contributes to loss of chemosensitivity). Because suppression of anoikis has been linked to tumor dormancy and metastatic spread of tumor cells (3 – 6), targeting anti-anoikis pathways may increase killing of primary tumor cells persisting in the circulation as anchorage-independent micrometastases during chemotherapy. For example, targeting the ErbB4 tyrosine kinase or its downstream pathways may reduce metastatic disease in ETs, but this awaits further studies.

Supplementary Material

Refer to Web version on PubMed Central for supplementary material.

Acknowledgments

Grant support: The Ronald A. and Victoria Mann Simms Foundation, the Fannie Ripple Foundation, the David Paul Kane Foundation, the Melanie Silverman Bone and Soft Tissue Fund, the Children's Oncology Group (P.H.B. Sorensen), and the National Childhood Cancer Foundation (P.H.B. Sorensen). W.A.M. is supported by NIH R01 CA90666.

We thank Dr. Stuart Siegel for support and helpful discussions.

References

1. Frisch SM, Screaton RA. Anoikis mechanisms. Curr Opin Cell Biol. 2001; 13:555–562. [PubMed: 11544023]
2. Ponten J. Spontaneous and virus induced transformation in cell culture. Virol Monogr. 1971; 8:1–253. [PubMed: 4354654]
3. Fidler IJ. The pathogenesis of cancer metastasis: the"seed and soil" hypothesis revisited. Nat Rev Cancer. 2003; 3:453–458. [PubMed: 12778135]

4. Douma S, Van Laar T, Zevenhoven J, Meuwissen R, Van Garderen E, Peeper DS. Suppression of anoikis and induction of metastasis by the neurotrophic receptor TrkB. Nature. 2004; 430:1034–1039. [PubMed: 15329723]
5. Demicheli R. Tumour dormancy: findings and hypotheses from clinical research on breast cancer. Semin Cancer Biol. 2001; 11:297–306. [PubMed: 11513565]
6. Naumov GN, MacDonald IC, Chambers AF, Groom AC. Olitary cancer cells as a possible source of tumour dormancy? Semin Cancer Biol. 2001; 11:271–276. [PubMed: 11513562]
7. Bissell MJ, Radisky D. Putting tumours in context. Nat Rev Cancer. 2001; 1:46–54. [PubMed: 11900251]
8. Yamada KM, Clark K. Cell biology: survival in three dimensions. Nature. 2002; 419:790–791. [PubMed: 12397336]
9. Weaver VM, Petersen OW, Wang F, et al. Reversion of the malignant phenotype of human breast cells in three-dimensional culture and *in vivo* by integrin blocking antibodies. J Cell Biol. 1997; 137:231–245. [PubMed: 9105051]
10. Weaver VM, Lelievre S, Lakins JN, et al. β4 Integrin-dependent formation of polarized three-dimensional architecture confers resistance to apoptosis in normal and malignant mammary epithelium. Cancer Cell. 2002; 2:205–216. [PubMed: 12242153]
11. Debnath J, Mills KR, Collins NL, Reginato MJ, Muthuswamy SK, Brugge JS. The role of apoptosis in creating and maintaining luminal space within normal and oncogene-expressing mammary acini. Cell. 2002; 111:29–40. [PubMed: 12372298]
12. Debnath J, Brugge JS. Modelling glandular epithelial cancers in three-dimensional cultures. Nat Rev Cancer. 2005; 5:675–688. [PubMed: 16148884]
13. Santini MT, Rainaldi G. Three-dimensional spheroid model in tumor biology. Pathobiology. 1999; 67:148–157. [PubMed: 10394136]
14. Bates RC, Edwards NS, Yates JD. Spheroids and cell survival. Crit Rev Oncol Hematol. 2000; 36:61–74. [PubMed: 11033297]
15. Rak J, Mitsuhashi Y, Erdos V, Huang SN, Filmus J, Kerbel RS. Massive programmed cell death in intestinal epithelial cells induced by three-dimensional growth conditions: suppression by mutant c-Hras oncogene expression. J Cell Biol. 1995; 131:1587–1598. [PubMed: 8522614]
16. St Croix B, Kerbel RS. Cell adhesion and drug resistance in cancer. Curr Opin Oncol. 1997; 9:549–556. [PubMed: 9370076]
17. Santini MT, Rainaldi G, Indovina PL. Apoptosis, cell adhesion and the extracellular matrix in the three-dimensional growth of multicellular tumor spheroids. Crit Rev Oncol Hematol. 2000; 36:75–87. [PubMed: 11033298]
18. Durand RE, Olive PL. Resistance of tumor cells to chemo- and radiotherapy modulated by the three-dimensional architecture of solid tumors and spheroids. Methods Cell Biol. 2001; 64:211–233. [PubMed: 11070841]
19. Hermiston ML, Gordon JI. *In vivo* analysis of cadherin function in the mouse intestinal epithelium: essential roles in adhesion, maintenance of differentiation, and regulation of programmed cell death. J Cell Biol. 1995; 129:489–506. [PubMed: 7721948]
20. Peluso JJ, Pappalardo A, Trolice MP. N-cadherin-mediated cell contact inhibits granulosa cell apoptosis in a progesteroneindependent manner. Endocrinology. 1996; 137:1196–203. Abstract. [PubMed: 8625889]
21. Rak J, Mitsuhashi Y, Sheehan C, et al. Collateral expression of proangiogenic and tumorigenic properties in intestinal epithelial cell variants selected for resistance to anoikis. Neoplasia. 1999; 1:23–30. [PubMed: 10935467]
22. Tran NL, Adams DG, Vaillancourt RR, Heimark RL. Signal transduction from N-cadherin increases Bcl-2. Regulation of the phosphatidylinositol 3-kinase/Akt pathway by homophilic adhesion and actin cytoskeletal organization. J Biol Chem. 2002; 277:32905–32914. [PubMed: 12095980]
23. Fouquet S, Lugo-Martinez VH, Faussat AM, et al. Early loss of Ecadherin from cell-cell contacts is involved in the onset of Anoikis in enterocytes. J Biol Chem. 2004; 279:43061–43069. [PubMed: 15292248]

24. Kantak SS, Kramer RH. E-Cadherin regulates anchorageindependent growth and survival in oral squamous cell carcinoma cells. J Biol Chem. 1998; 273:16953–16961. [PubMed: 9642258]
25. Lawlor ER, Scheel C, Irving J, Sorensen PHB. Anchorageindependent multi-cellular spheroids as an *in vitro* model of growth signaling in Ewing tumors. Oncogene. 2002; 21:307–318. [PubMed: 11803474]
26. Zhang J, Hu S, Schofield DE, Sorensen PH, Triche TJ. Selective usage of D-type cyclins by Ewing's tumors and rhabdomyosarcomas. Cancer Res. 2004; 64:6026–6034. [PubMed: 15342383]
27. Sorensen PHB, Liu XF, Thomas G, et al. Reverse transcriptase PCR amplification of EWS/Fli-1 fusion transcripts as a diagnostic test for peripheral primitive neuroectodermal tumors of childhood. Diagn Mol Pathol. 1993; 2:147–157. [PubMed: 7506981]
28. Martin MJ, Melnyk N, Pollard M, et al. The insulin-like growth factor I receptor is required for Akt activation and suppression of anoikis in cells transformed by the ETV6-NTRK3 chimeric tyrosine kinase. Mol Cell Biol. 2006; 26:1754–1769. [PubMed: 16478996]
29. Keshelava N, Frgala T, Krejsa J, Kalous O, Reynolds CP. DIMSCAN: a microcomputer fluorescence-based cytotoxicity assay for preclinical testing of combination chemotherapy. Methods Mol Med. 2005; 110:139–153. [PubMed: 15901933]
30. Zhu AJ, Watt FM. Expression of a dominant negative cadherin mutant inhibits proliferation and stimulates terminal differentiation of human epidermal keratinocytes. J Cell Sci. 1996; 109:3013–3023. Abstract. [PubMed: 9004036]
31. Cavallaro U, Christofori G. Cell adhesion and signalling by cadherins and Ig-CAMs in cancer. Nat Rev Cancer. 2004; 4:118–132. [PubMed: 14964308]
32. Tognon C, Garnett M, Kenward E, Kay R, Morrison K, Sorensen PH. The chimeric protein tyrosine kinase ETV6-NTRK3 requires both Ras-Erk1/2 and PI3-kinase-Akt signaling for fibroblast transformation. Cancer Res. 2001; 61:8909–8916. [PubMed: 11751416]
33. Maatta JA, Sundvall M, Junttila TT, et al. Proteolytic cleavage and phosphorylation of a tumor-associated ErbB4 isoform promote ligand-independent survival and cancer cell growth. Mol Biol Cell. 2006; 17:67–79. [PubMed: 16251361]
34. Vivanco I, Sawyers CL. The phosphatidylinositol 3-kinase AKT pathway in human cancer. Nat Rev Cancer. 2002; 2:489–501. [PubMed: 12094235]
35. Kemler R, Ozawa M, Ringwald M. Calcium-dependent cell adhesion molecules. Curr Opin Cell Biol. 1989; 1:892–897. [PubMed: 2697291]
36. Ni CY, Murphy MP, Golde TE, Carpenter G. γ-Secretase cleavage and nuclear localization of ErbB-4 receptor tyrosine kinase. Science. 2001; 294:2179–2181. [PubMed: 11679632]
37. Lee HJ, Jung KM, Huang YZ, et al. Presenilin-dependent γ- secretase-like intramembrane cleavage of ErbB4. J Biol Chem. 2002; 277:6318–6323. [PubMed: 11741961]
38. Linggi B, Cheng QC, Rao AR, Carpenter G. The ErbB-4 s80 intracellular domain is a constitutively active tyrosine kinase. Oncogene. 2005; 25:160–163. [PubMed: 16170367]
39. Plowman GD, Culouscou JM, Whitney GS, et al. Ligand-specific activation of HER4/p180erbB4, a fourth member of the epidermal growth factor receptor family. Proc Natl Acad Sci U S A. 1993; 90:1746–1750. [PubMed: 8383326]
40. Guo G, Wang T, Gao Q, et al. Expression of ErbB2 enhances radiation-induced NF-κB activation. Oncogene. 2004; 23:535–545. [PubMed: 14724581]
41. Grossmann J. Molecular mechanisms of “detachment-induced apoptosis-Anoikis”. Apoptosis. 2002; 7:247–260. [PubMed: 11997669]
42. White DE, Rayment JH, Muller WJ. Addressing the role of cell adhesion in tumor cell dormancy. Cell Cycle. 2006; 5:1756–1759. [PubMed: 16880738]
43. Sato H, Hasegawa T, Abe Y, Sakai H, Hirohashi S. Expression of E-cadherin in bone and soft tissue sarcomas: a possible role in epithelial differentiation. Hum Pathol. 1999; 30:1344–1349. [PubMed: 10571515]
44. Schuetz AN, Rubin BP, Goldblum JR, et al. Intercellular junctions in Ewing sarcoma/primitive neuroectodermal tumor: additional evidence of epithelial differentiation. Mod Pathol. 2005; 18:1403–1410. [PubMed: 15920547]

45. Sanceau J, Truchet S, Bauvois B. Matrix metalloproteinase-9 silencing by RNA interference triggers the migratory-adhesive switch in Ewing's sarcoma cells. J Biol Chem. 2003; 278:36537–36546. [PubMed: 12847101]
46. Tirado OM, Mateo-Lozano S, Villar J, et al. Caveolin-1 (CAV1) is a target of EWS/FLI-1 and a key determinant of the oncogenic phenotype and tumorigenicity of Ewing's sarcoma cells. Cancer Res. 2006; 66:9937–9947. [PubMed: 17047056]
47. Andrews NA, Jones AS, Helliwell TR, Kinsella AR. Expression of the E-cadherin-catenin cell adhesion complex in primary squamous cell carcinomas of the head and neck and their nodal metastases. Br J Cancer. 1997; 75:1474–1480. [PubMed: 9166940]
48. Auersperg N, Pan J, Grove BD, et al. E-Cadherin induces mesenchymal-to-epithelial transition in human ovarian surface epithelium. Proc Natl Acad Sci U S A. 1999; 96:6249–6254. [PubMed: 10339573]
49. Sundfeldt K. Cell-cell adhesion in the normal ovary and ovarian tumors of epithelial origin; an exception to the rule. Mol Cell Endocrinol. 2003; 202:89–96. [PubMed: 12770736]
50. Reddy P, Liu L, Ren C, et al. Formation of E-cadherin-mediated cell-cell adhesion activates AKT and mitogen activated protein kinase via phosphatidylinositol 3 kinase and ligand-independent activation of epidermal growth factor receptor in ovarian cancer cells. Mol Endocrinol. 2005; 19:2564–2578. [PubMed: 15928314]
51. Ong A, Maines-Bandiera SL, Roskelley CD, Auersperg N. An ovarian adenocarcinoma line derived from SV40/E-cadherintransfected normal human ovarian surface epithelium. Int J Cancer. 2000; 85:430–437. [PubMed: 10652437]
52. Warren CM, Landgraf R. Signaling through ERBB receptors: multiple layers of diversity and control. Cell Signal. 2006; 18:923–933. [PubMed: 16460914]
53. Gullick WJ. c-erbB-4/HER4: friend or foe? J Pathol. 2003; 200:279–281. [PubMed: 12845622]
54. Junttila TT, Sundvall M, Lundin M, et al. Cleavable ErbB4 isoform in estrogen receptor-regulated growth of breast cancer cells. Cancer Res. 2005; 65:1384–1393. [PubMed: 15735025]
55. Starr A, Greif J, Vexler A, et al. ErbB4 increases the proliferation potential of human lung cancer cells and its blockage can be used as a target for anti-cancer therapy. Int J Cancer. 2006; 119:269–274. [PubMed: 16463386]
56. Sartor CI, Zhou H, Kozlowska E, et al. Her4 mediates liganddependent antiproliferative and differentiation responses in human breast cancer cells. Mol Cell Biol. 2001; 21:4265–4275. [PubMed: 11390655]
57. Naresh A, Long W, Vidal GA, et al. The ERBB4/HER4 intracellular domain 4ICD is a BH3-only protein promoting apoptosis of breast cancer cells. Cancer Res. 2006; 66:6412–6420. [PubMed: 16778220]
58. Shen X, Kramer RH. Adhesion-mediated squamous cell carcinoma survival through ligand-independent activation of epidermal growth factor receptor. Am J Pathol. 2004; 165:1315–1329. [PubMed: 15466396]
59. Pece S, Gutkind JS. Signaling from E-cadherins to the MAPK pathway by the recruitment and activation of epidermal growth factor receptors upon cell-cell contact formation. J Biol Chem. 2000; 275:41227–41233. [PubMed: 10969083]
60. Zantek ND, Azimi M, Fedor-Chaiken M, Wang B, Brackenbury R, Kinch MS. E-Cadherin regulates the function of the EphA2 receptor tyrosine kinase. Cell Growth Differ. 1999; 10:629–638. [PubMed: 10511313]
61. Zhang W, Zong CS, Hermanto U, Lopez-Bergami P, Ronai Z, Wang LH. RACK1 recruits STAT3 specifically to insulin and insulinlike growth factor 1 receptors for activation, which is important for regulating anchorage-independent growth. Mol Cell Biol. 2006; 26:413–424. [PubMed: 16382134]
62. Mueller S, Cadenas E, Schonthal AH. p21WAF1 regulates anchorage-independent growth of HCT116 colon carcinoma cells via E-cadherin expression. Cancer Res. 2000; 60:156–163. [PubMed: 10646868]

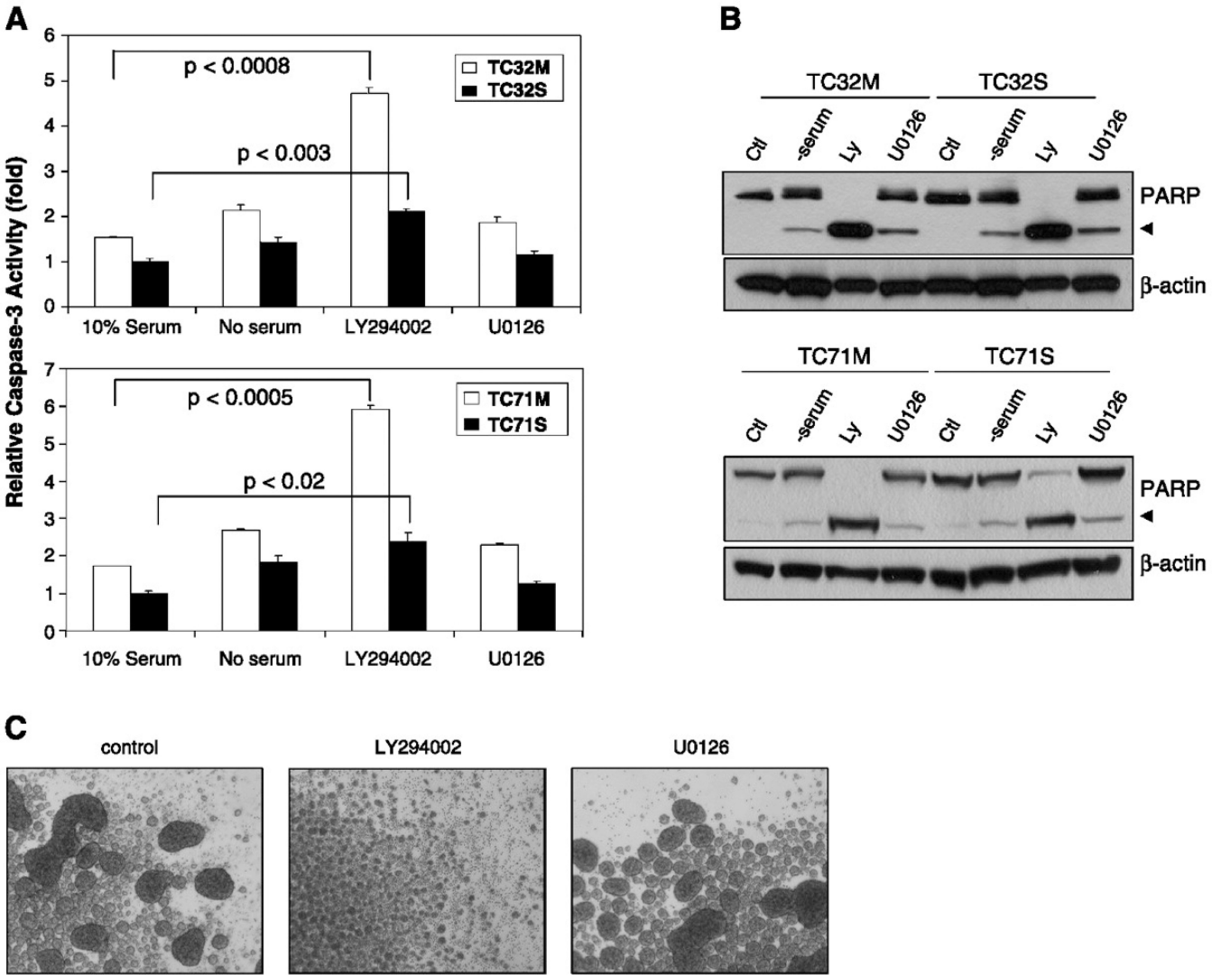

Figure 1.

Suppression of anoikis in ET multicellular spheroids is blocked by PI3K inhibition. *A*, TC32 and TC71 ET spheroids were grown in 10% serum media, serum-free media, or 10% serum media containing 20 μmol/L LY294002 or 30 μmol/L U0126 for 24 h. After adjustment for protein concentration, caspase-3 activity was measured by fluorometry as described in Materials and Methods, and normalized to a value of 1.0 arbitrary unit for spheroid cells in 10% serum. Statistical analysis of data from at least three separate experiments was done using Student's *t* test. *Horizontal lines*, *P* values comparing 10% serum ± LY294002 treatment for TC32 monolayers (*TC32M*; $P < 0.0008$), TC32 spheroids (*TC32S*; $P < 0.003$), TC71 monolayers (*TC71M*; $P < 0.0005$), and TC71 spheroids (*TC71S*; $P < 0.02$). *B*, lysates from the same TC32 and TC71 ET spheroids or monolayers were assayed for poly(ADP-ribose) polymerase (*PARP*) cleavage by Western blotting after 24 h growth in 10% serum media (*Ctl*), serum-free media (−*serum*), or in 10% serum media containing 20 μmol/L LY294002 (*Ly*) or 30 μmol/L U0126 (*U0126*). *Arrowhead*, cleaved poly(ADP-ribose) polymerase. β-Actin was used as a loading control. *C*, effects of the PI3K inhibitor LY294002 (20 μmol/L) or the MEK inhibitor U0126 (30 μmol/L) on ET spheroid formation. TC32 cells were treated with agents or vehicle control for 15 h following transfer of monolayer cells to agar-coated plates.

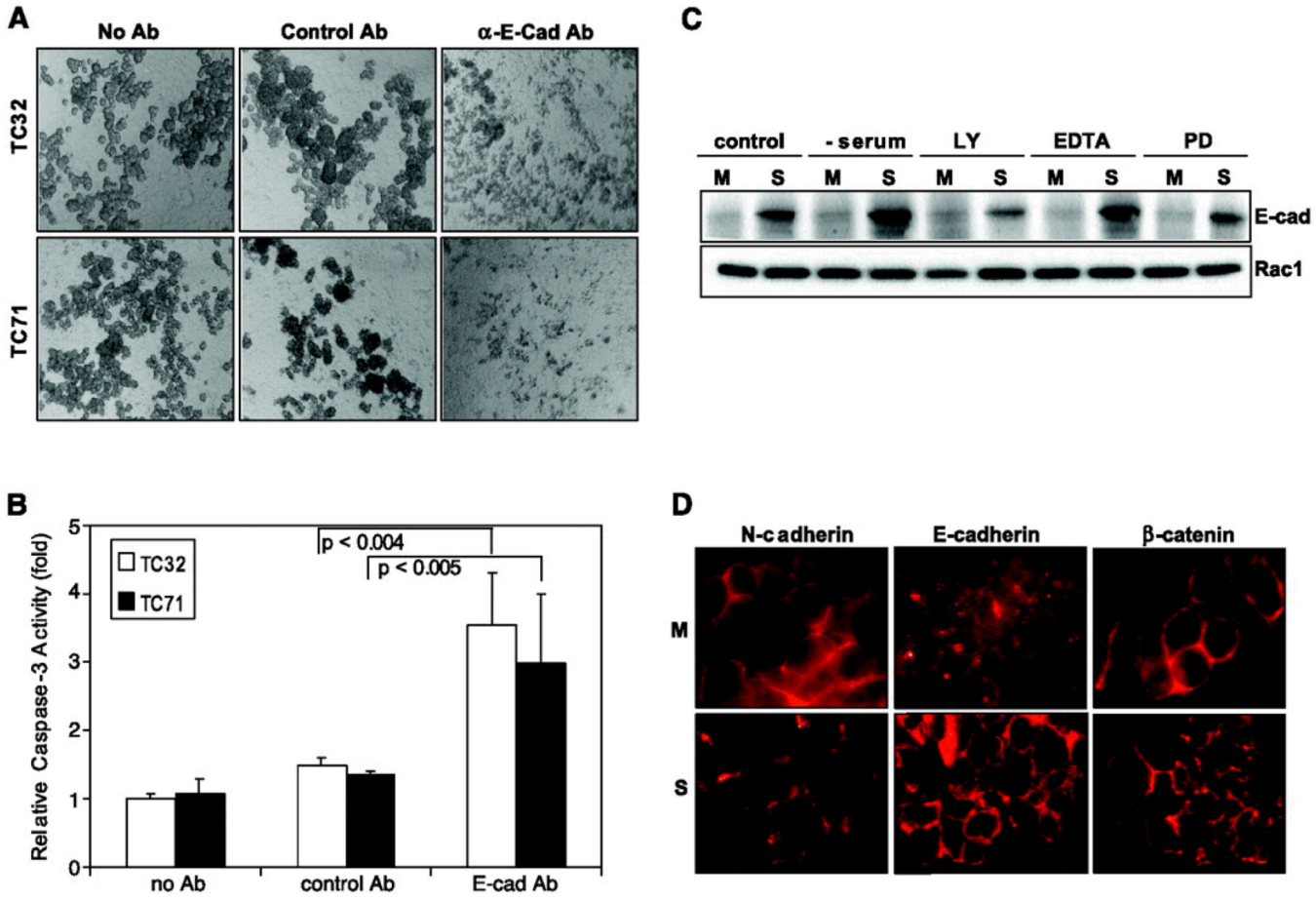

Figure 2.

Anti–E-cadherin antibodies block the formation of ET spheroids and E-cadherin expression is up-regulated in ET spheroids. *A*, TC32 and TC71 ET cells were plated on agar-coated plates in the presence and absence of anti–E-cadherin or control IgG antibodies (*Ab*), grown for 48 h, and then photographed using a phase-contrast microscope (magnification, ×40). *B*, TC32 and TC71 cells were grown on agar-coated plates ± anti–E-cadherin or control IgG antibodies for 48 h, lysed, and assayed for caspase-3 activity by fluorometry as described in Materials and Methods. Caspase-3 activity was normalized to a value of 1.0 arbitrary unit for control cells in the absence of antibodies. Statistical analysis of data from three separate experiments was done using Student's *t* test. *Horizontal lines*, *P* values comparing control versus E-cadherin antibodies for TC32 spheroids ($P < 0.004$) or TC71 spheroids ($P < 0.005$). *C*, TC32 cells were grown in monolayer (*M*) versus spheroid (*S*) cultures in media containing 10% serum (*control*), in serum-free media (−*serum*), or 10% serum media containing LY294002 (*LY*; 20 μmol/L), EDTA (2.5 mmol/L), or the MEK inhibitor PD98059 (*PD*; 50 μmol/L) for 24 h. Cells were then lysed and subjected to immunoblotting with anti–E-cadherin antibodies. Detection of Rac1 by immunoblotting was used as a loading control. *D*, monolayer and spheroid TC32 cell cultures were subjected to immunofluorescence staining with anti–N-cadherin, anti–E-cadherin, or anti–β-catenin antibodies as described in Materials and Methods. Magnification, ×100.

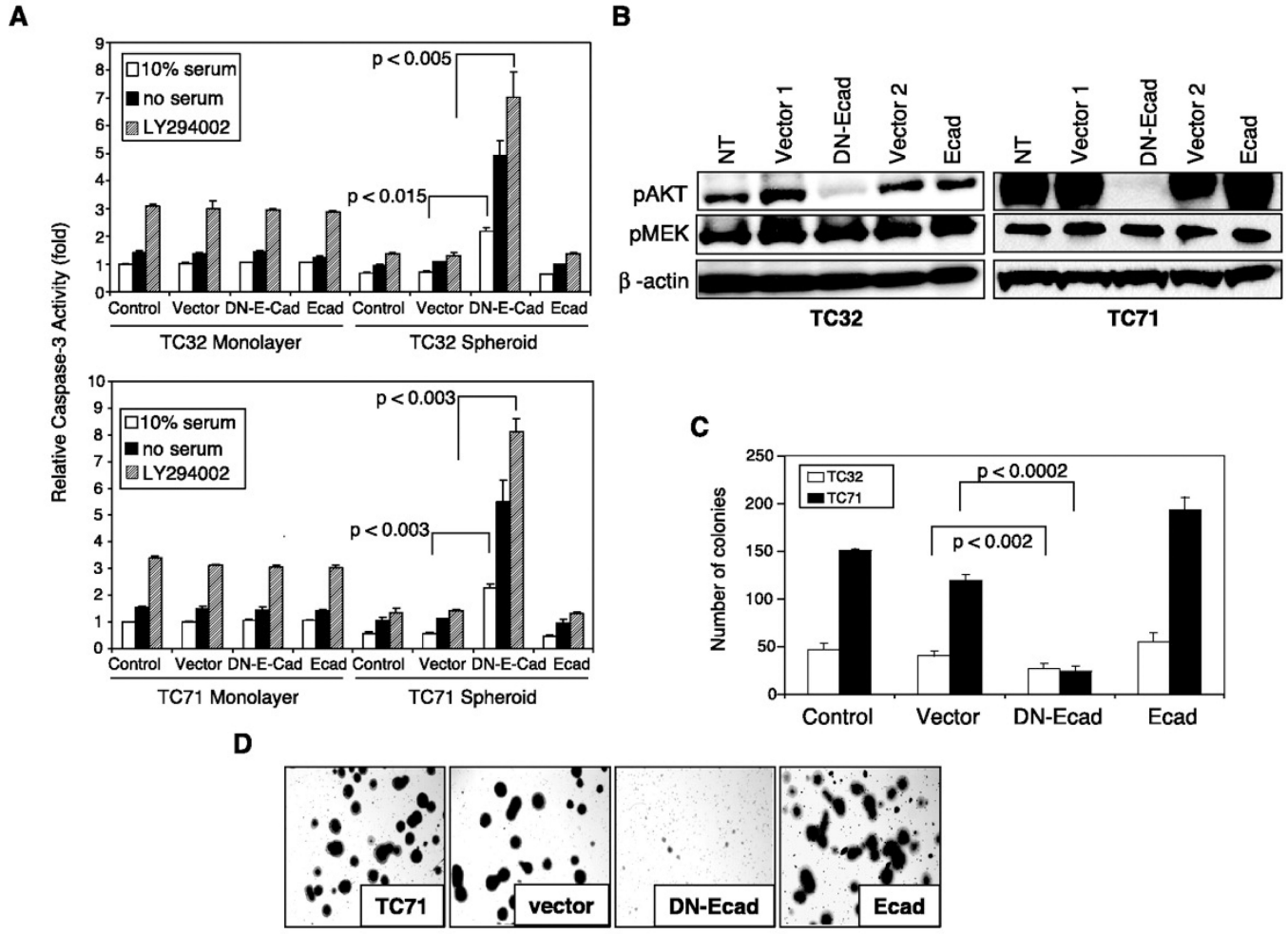

Figure 3.

E-cadherin expression levels influence survival, soft agar formation, and Akt activation of anchorage-independent ET cells. *A*, TC32 cells (*top*) or TC71 cells (*bottom*) that were nontransduced (*Control*), transduced with vector alone (*Vector*), or stably expressing DN-Ecad or Ecad were grown as monolayers or spheroids in 10% serum for 30 h. Cells were then transferred to fresh 10% serum, serum-free medium (*no serum*), or 10% serum plus 20 μmol/L LY294002 as indicated for a further 24 h. Cells were then lysed and assayed for caspase-3 activity by fluorometry as described in Materials and Methods. The relative caspase-3 activity was normalized to a value of 1.0 for TC32 (*top*) and TC71 monolayers (*bottom*) grown in 10% serum. Statistical analysis of data from at least three separate experiments was done using Student's *t* test. *Horizontal lines*, *P* values comparing vector alone versus DN-Ecad TC32 spheroids in 10% serum ($P < 0.015$) or in 10% serum plus 20 μmol/L LY294002 ($P < 0.005$; *top*), and comparing vector alone versus DN-Ecad TC71 spheroids in 10% serum ($P < 0.003$) or in 10% serum plus 20 μmol/L LY294002 ($P < 0.003$; *bottom*). No significant differences were observed comparing monolayer TC32 or TC71 vector cells with DN-Ecad cells, either with or without LY294002 treatment (data not shown). *B*, TC32 and TC71 cell lines that were either nontransduced (*NT*), stably expressing DN-Ecad or vector alone (*Vector 1*), or stably expressing Ecad or vector alone (*Vector 2*) were grown on agar-coated dishes in 10% serum–containing media for 48 h. Cells were then starved for 24 h in 0.1% serum followed by stimulation with 10% serum for 30 min. Cells were then lysed and subjected to immunoblotting with antibodies to phospho-Akt and

phospho-MEK. Detection of β-actin was used as a loading control. *C*, nontransduced TC32 and TC71, vector control, DN-Ecad–expressing, and Ecad-expressing cells were resuspended in a top layer of 0.2% agar in 10% fetal bovine serum, overlying a layer of 0.4% agar in Iscove's modified Dulbecco's medium and 20% fetal bovine serum as described in Materials and Methods. After 14 d, the average number of colonies per well was counted. Statistical analysis was done with Student's *t* test on representative results of at least three independent assays for each cell line. *Horizontal lines*, *P* values comparing soft agar colony formation after 14 d for vector alone versus DN-Ecad TC32 cells ($P < 0.002$) and TC71 cells ($P < 0.0002$). *D*, soft agar colonies for control, vector alone, DN-Ecad–, and Ecad-expressing TC71 cells were photographed after 14 d (magnification, ×40).

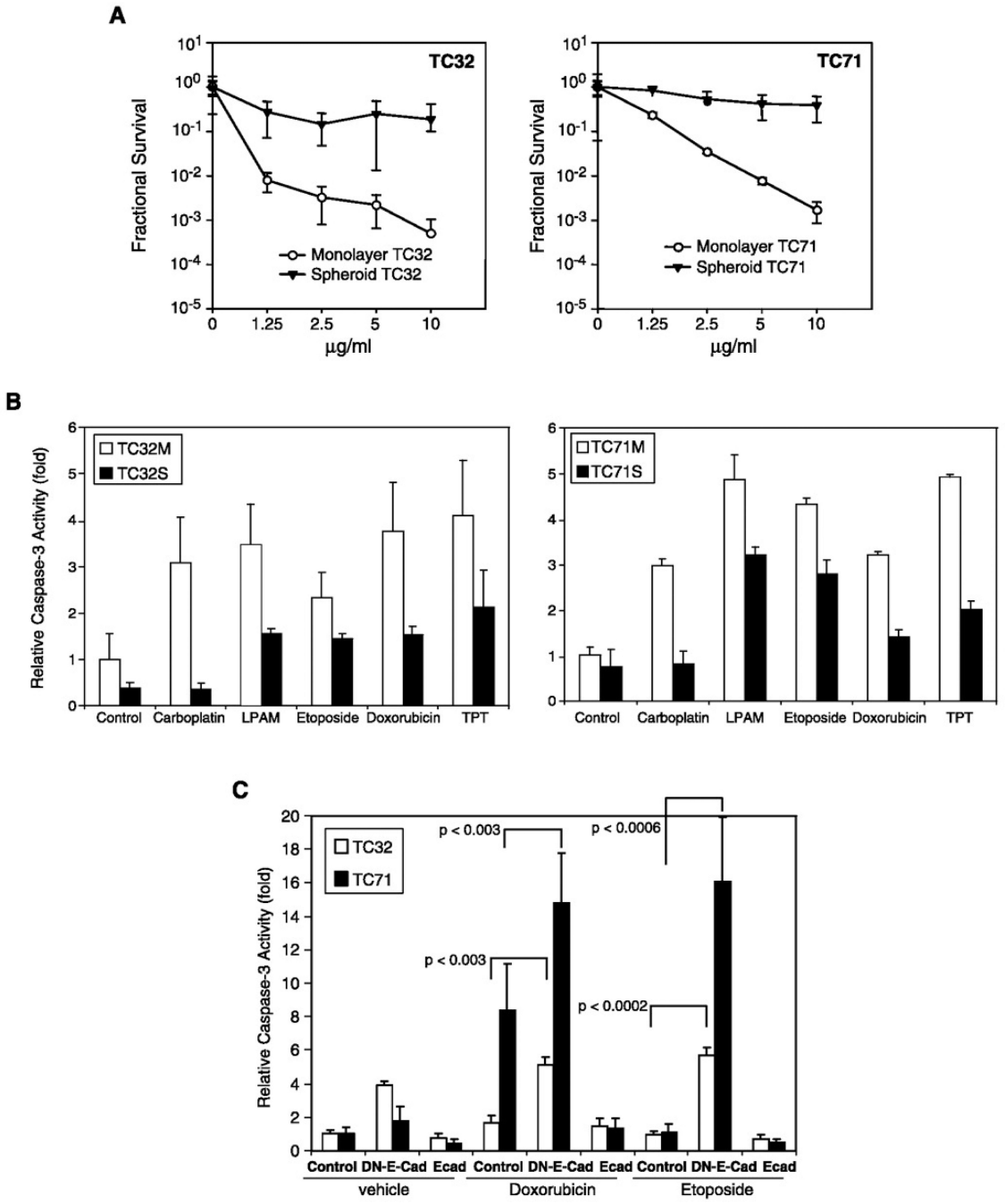

Figure 4.

ET spheroids show increased resistance to drug treatment. *A*, dose-response curves of fractional survival of TC32 and TC71 monolayer (○) or spheroid cells (□) in the presence of carboplatin. TC32 and TC71 ET cells were grown in 96-well plates as monolayer cultures or poly-2-hydroxyethyl methacrylate–coated plates as spheroids for 24 h and then treated with increasing concentrations (in µg/mL) of carboplatin for 5 d in media containing 10% serum. Fractional survival (cytotoxicity) profiles were determined by DIMSCAN analysis as described in Materials and Methods. *B*, caspase-3 activity of TC32 and TC71 ET monolayer versus spheroid cultures in the presence of anticancer drugs. Spheroids and subconfluent monolayer cells were grown for 24 h in 10% serum and then cultured in the presence of

vehicle control, carboplatin (5 μg/mL), melphalan (*LPAM*; 5 μg/mL), etoposide (50 μmol/L), doxorubicin (10 μmol/L), or topotecan (*TPT*; 5 μg/mL) for a further 24 h. Caspase-3 activity of cell lysates was then measured by fluorometry as described in Materials and Methods after adjustment for protein concentration. Caspase-3 activity was normalized to a value of 1.0 arbitrary unit for vehicle control monolayer cells. Representative results of at least three independent assays for each cell line. Statistical analysis was done using Student's *t* test and showed significantly higher caspase-3 activation ($P < 0.005$ or lower) in ET monolayers compared with spheroids for both cell lines and for each drug treatment (data not shown). *C*, dominant negative E-cadherin expression restores chemosensitivity of ET spheroids. TC32 and TC71 vector control, DN-Ecad–, and Ecad-expressing cells were grown on agar-coated plates in media containing 10% serum and vehicle control, 10 μmol/L doxorubicin, or 50 μmol/L etoposide for 24 h. Spheroids were then lysed and assayed for caspase-3 activity by fluorometry as described. Caspase-3 activity was normalized to a value of 1.0 arbitrary unit for vehicle control cells in the absence of drug treatment. Statistical analysis of data from at least three separate experiments was done using Student's *t* test. *Horizontal lines*, *P* values comparing vector control versus DN-Ecad TC32 spheroids after doxorubicin ($P < 0.003$) or etoposide treatment ($P < 0.0002$), and comparing vector control versus DN-Ecad TC71 spheroids after doxorubicin ($P < 0.003$) or etoposide treatment ($P < 0.0006$).

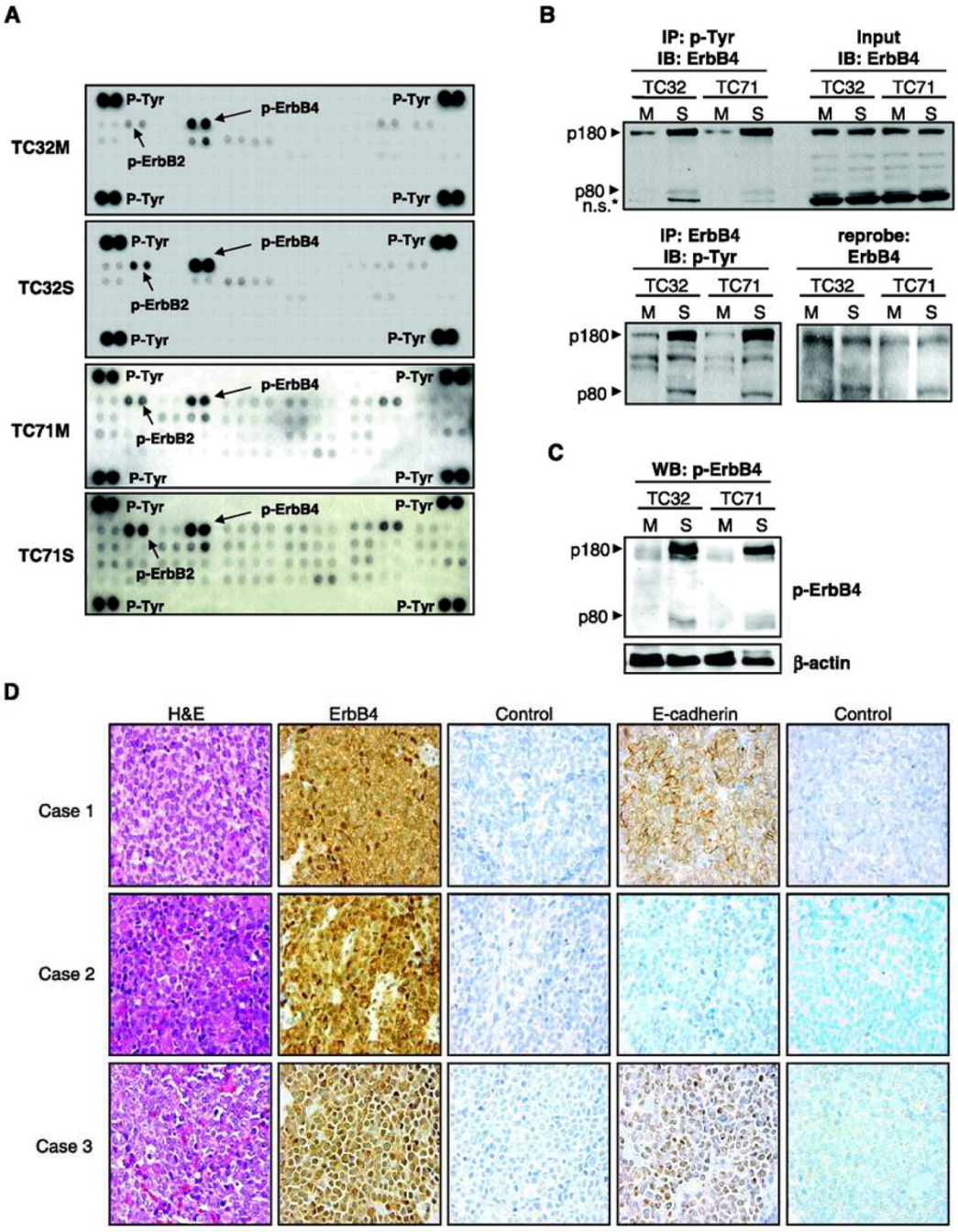

Figure 5.

Activation of the ErbB4 RTK in ET spheroids. *A*, the R&D Systems Human Phospho-RTK Antibody Proteome Profiler Array system was used to screen for activation of specific tyrosine kinases in ET spheroids. Lysates from TC32 and TC71 monolayer and spheroid cultures were incubated with membranes arrayed with antibodies from 42 different tyrosine kinases (http://www.rndsystems.com/). Membranes were then washed and incubated with anti–phosphotyrosine-HRP antibodies followed by enhanced chemiluminescence detection to identify activated tyrosine kinases. *P-Tyr*, phospho-tyrosine control spots. *B, top*, lysates from TC32 and TC71 monolayer and spheroid cultures were subjected to immunoprecipitation (*IP*) with 4G10 anti-phosphotyrosine antibodies and then

immunoblotted (*IB*) with an anti-ErbB4 antibody. The positions of 180- and 80-kDa tyrosine phosphorylated species are indicated. *n.s.*, nonspecific band. *Left*, lysates from TC32 and TC71 monolayer and spheroid cultures were subjected to immunoprecipitation with antibodies to total ErbB4 followed by immunoblotting with anti-phosphotyrosine antibodies. *Right*, the blot was then reprobed with an anti-ErbB4 antibody. The positions of 180- and 80-kDa tyrosine phosphorylated species are indicated. *C*, TC32 and TC71 cells were grown as monolayers or spheroids as indicated in 10% serum–containing media for 48 h. Cells were then lysed and subjected to immunoblotting with antibodies to activated ErbB4 (phospho-Tyr^{1188}). Detection of β-actin was used as a loading control. The positions of 180- and 80-kDa tyrosine phosphorylated species are indicated. *D*, ErbB4 and E-cadherin expression was analyzed by immunohistochemistry from sections from primary ET. Sections were subjected to standard H&E staining, as well as immunohistochemistry with anti-ErbB4 (*ErbB4*), anti–E-cadherin, and control IgG antibodies. Magnification, ×400.

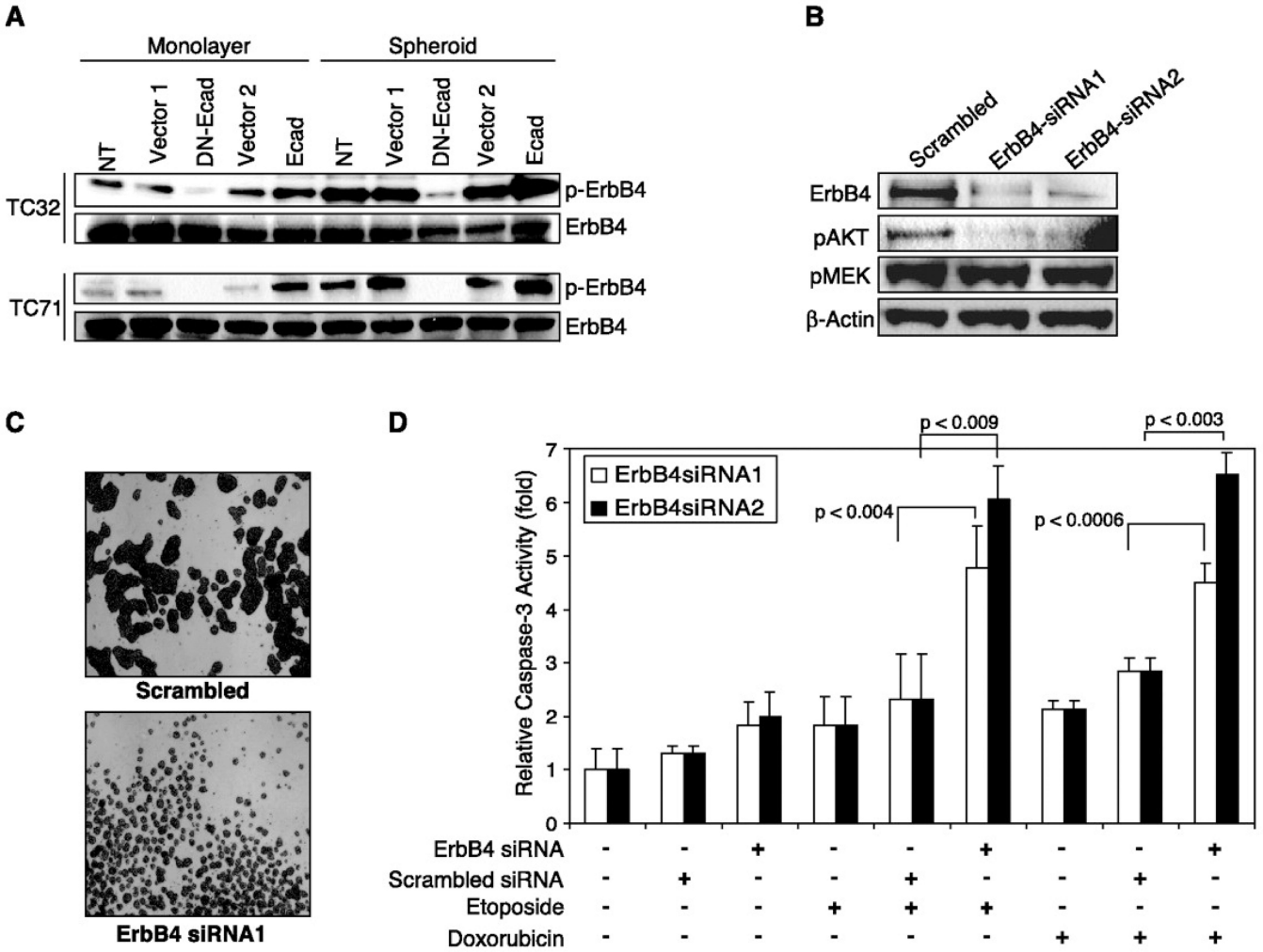

Figure 6.

ErbB4 RNA interference blocks Akt activation and restores chemosensitivity of ET spheroids. *A*, TC32 and TC71 cell lines that were either nontransduced or stably expressing DN-Ecad or its vector alone or Ecad or its vector alone were grown as monolayers or spheroids as indicated in 10% serum–containing media for 48 h. Cells were then lysed and subjected to immunoblotting with antibodies to activated ErbB4 (phospho-Tyr^{1188}; *p-ErbB4*) or total ErbB4. *B*, ErbB4 knockdown with RNA interference blocks Akt activation. TC32 spheroids grown in media containing 10% serum were treated with two ErbB4-specific siRNA pools (siRNA1 or siRNA2), as described in Materials and Methods, or a scrambled siRNA control. Lysates were then subjected to immunoblotting with antibodies to total ErbB4, phospho-Akt (*pAKT*), phospho-MEK (*pMEK*), or β-actin as a loading control. *C*, phase-contrast photomicrographs of TC32 spheroids after pretreatment of cells with an ErbB4-specific siRNA (siRNA1) or a scrambled siRNA control. Magnification, ×40.*D*, reduction of ErbB4 by RNA interference restores chemosensitivity of ET spheroids. TC32 spheroids grown in media containing 10% serum were treated with ErbB4-specific siRNAs or a scrambled control as above. Cells were then treated with vehicle control, 50 μmol/L etoposide, or 10 μmol/L doxorubicin for 24 h after siRNA transfection. Caspase-3 activity was then assayed as above with normalization to a value of 1.0 arbitrary unit for nontreated cells. Statistical analysis of data from at least three separate experiments was done using Student's *t* test. *Horizontal lines*, *P* values comparing scrambled siRNA control with ErbB4

siRNA1 cells in the presence of etoposide ($P < 0.004$) or doxorubicin ($P < 0.009$), or comparing scrambled siRNA control with ErbB4 siRNA2 in the presence of etoposide ($P < 0.0006$) or doxorubicin ($P < 0.003$).